Mathematical Modelling and Control

https://www.aimspress.com/journal/mmc

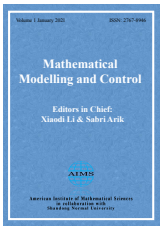

MMC, 5(2): 202–215.
DOI: 10.3934/mmc.2025015
Received: 22 April 2024
Revised: 18 August 2024
Accepted: 17 October 2024
Published: 09 June 2025

Research article

Partial-nodes-based state estimation for complex networks under hybrid attacks: a dynamic event-triggered approach

Lu Zhou, Jin Hu and Bing Li*

School of Mathematics and Statistics, Chongqing Jiaotong University, Chongqing 400074, China

* **Correspondence:** Email: bingli@cqjtu.edu.cn.

Abstract: This article addresses the problem of state estimation for complex networks under hybrid cyber attacks. A hybrid model is constructed to encompass cyber attacks in both deception and denial-of-service (DoS) manners. A dynamic event-triggered mechanism (DETM) is brought into the channel between sensors and the estimator for deducing the transmission frequency. Our primary target is to develop an estimator capable of accurately assessing network states, relying on measurements from partially selected network nodes. Taking use of Lyapunov stability theory and stochastic analysis techniques, several criteria are formulated to guarantee the exponentially mean square ultimate boundedness (EMSUB) of the estimation error dynamics. The estimator gains are determined by resolving specific matrix inequalities. To illustrate the efficacy of our newly devised estimator design approach, a numerical example is provided along with corresponding simulations.

Keywords: complex networks (CNs); hybrid attacks; partial-nodes-based state estimation; dynamic event-triggered mechanism

1. Introduction

Complex networks (CNs), which are large-scale systems consisting of numerous nodes interconnected by edges in specific topological arrangements, create a highly interdependent and dynamic network framework [1]. These networks effectively represent a variety of real-world systems, including sensor networks, neural networks, and biological networks, cited in the literature as references [2, 3], and [4], respectively. In recent years, CNs have attracted substantial attention in the fields of intelligent control and system science, as referenced in [5–7]. Among the various research areas, the focus on stability and synchronization of CNs has been particularly notable, as highlighted in studies [8–12].

The analysis of CNs relies heavily on state information to decipher their intrinsic structures. However, the acquisition of precise state data in CNs poses a challenge due to issues such as their extensive scale, intricate interconnections between nodes, and uncertainties in their models [13–19]. Addressing the state estimation challenge in CNs, where only limited measurements are accessible, is crucial for comprehending their dynamic properties. State estimation involves deducing the internal states of network entities using these available data points. This issue has garnered considerable attention from the research community, leading to the development of various robust estimation methodologies. Notably, the H_∞ estimation approach focuses on meeting specific performance criteria in the error dynamics of estimation [17]. Another prominent technique is the Kalman estimation method, designed for time-varying CNs. The target of this study is to establish a recursive estimator to minimize the error variance [19]. These methodologies have been pivotal in advancing state estimation in CNs, offering deeper insights into their dynamics and aiding in a more profound understanding of their fundamental network structures.

Existing research on state estimation in CNs often

presupposes complete access to measurement data from all network nodes. Nevertheless, in practical situations, this presumption might not be applicable owing to the substantial expense to surveil and sample the complete measurements from a large number of network nodes. Besides, sensors may fail to measure and transmit the signal because of the limitation of communication resources. Additionally, considering the vulnerability of communication networks, the cyber attacks may also cause some of the measurements to be unobtainable by blocking the transmission channel. Given these practical limitations, it becomes vital to explore state estimation strategies that do not rely on data from all nodes. This leads to the concept of partial-nodes-based state estimation (PNBSE), a notion initially introduced in [20]. By utilizing the interdependencies among network nodes and the principle of partial observability, PNBSE posits that the states of unmonitored nodes can be inferred from the available data of the observed ones. Using a subset of nodes for state estimation can offer an effective and precise understanding of the general network dynamics in large-scale CNs, as indicated in references [21–25]. Despite the practical relevance of PNBSE, the literature on this topic remains fragmented. Our study attempts to bridge this gap by offering an extensive analysis of this nascent field.

The evolution of network communication technologies has introduced complexities in managing finite computational resources and shared bandwidth, particularly in sensor-limited networked systems. A common challenge in such environments is bandwidth constraints, often leading to time delays and packet losses. These issues require a strategic reduction in data transmission frequency to conserve network resources. To this end, event-triggered mechanisms (ETMs) have emerged as a solution, transmitting data only when specific conditions are met, as outlined in [26, 27]. This approach skillfully balances resource usage and system performance. ETMs can be categorized into static event-triggered mechanisms (SETMs) [28, 29] and dynamic event-triggered mechanisms (DETMs) [30–33]. SETMs operate with fixed threshold parameters, whereas DETMs dynamically adjust these thresholds using auxiliary variables. Recently, DETMs have advanced significantly, becoming increasingly favored for their efficient resource utilization and adaptability, surpassing traditional periodic triggering methods [34]. Integration into network system communications is crucial to improve resource management. However, in the context of CNs, the application of DETMs to PNBSE has not been extensively explored. This gap in the literature forms the primary impetus for our current research, with the aim of examining the problem of PNBSE under DETMs [35–39].

In networked systems, information transmission is pivotal for operational efficiency. Yet, this process is susceptible to cyber threats aimed at impairing network performance [40–43]. Key threats include deception attacks [44], DoS attacks [45, 46], and replay attacks [47]. Deception attacks compromise the integrity of the data, making it difficult to differentiate between true and false information. A DoS attack can interdict the signal transmissions to cause data missing. Notably, attackers often alternate between different attack types, enhancing their disruptive impact. This tactic complicates network analysis and design, posing additional challenges. Although extensive research has been undertaken regarding state estimation in CNs impacted by hybrid cyberattacks [48–52], the majority of these studies have focused primarily on singular systems. Our paper expands this scope to encompass CN security more broadly, integrating the DETM. The aim is two-fold: to optimize the usage of network resources and to strengthen defenses against cyber threats while maintaining system performance.

Taking into account the preceding discussions, this paper aims to examine the challenge of PNBSE in a specific type of CN, which is vulnerable to hybrid attacks, utilizing a DETM. This paper's principal contributions are outlined below:

(1) A hybrid model consisting of DoS and deception attacks is constructed to accurately describe the complexities of real attacks.
(2) The DETM with a variable threshold is designed in the channel between sensor nodes and estimator for the aim of conserving communication resources.
(3) An innovative PNBSE problem is addressed in the context of CNs with considering both network resource demand and the efficiency of state estimation under cyber attacks.

The remainder of this paper is structured as follows: Sec. 2 presents the CN model and outlines the formulation of the problem. Sec. 3 details the main contributions of this

paper. An illustrative simulation to showcase the theoretical results is provided in Sec. 4, while Sec. 5 concludes this paper.

Notations: In this study, we define the inverse and transpose of a matrix A as A^{-1} and A^T, respectively. $A > 0$ or $A < 0$ implies that A is a positive or negative definite matrix, respectively. $\mathbb{R}^n$ denotes the n-dimensional Euclidean space, and $\mathbb{R}^{n\times m}$ denotes the set of all $n\times m$ real matrices. The norm of a Euclidean vector is indicated as $|\cdot|$. $\mathbb{E}A$ represents the expected value of a random variable A. A block diagonal matrix is denoted by diag$\{\cdot\}$. For a symmetric matrix P, its minimum and maximum eigenvalues are signified by $\lambda_{min}(P)$ and $\lambda_{max}(P)$, respectively. The symbol $\otimes$ is used to denote the Kronecker product. The set of nonnegative integers is represented by $\mathbb{N}$. The likelihood of an event is expressed as $Prob\{\cdot\}$. Last, I denotes the identity matrix, appropriately dimensioned for the context.

2. Model description and preliminaries

Consider the discrete CNs with N coupled nodes as follows:

$$x_i(k+1) = A_i x_i(k) + B_i x_i(k-\tau(k)) + f(x_i(k)) + \sum_{j=1}^{N} w_{ij}\Gamma x_j(k) + L_i v_i(k), \quad i = 1, 2, \ldots, N, \quad (2.1)$$

where $x_i(k) = [x_{i1}(k) \quad x_{i2}(k) \quad \cdots \quad x_{in}(k)]^T \in \mathbb{R}^n$ denotes the state vector of the ith node. The discrete time-varying delay, represented by the positive integer $\tau(k)$, adheres to $0 < \tau_1 \leq \tau(k) \leq \tau_2$ with τ_1, τ_2 being positive integers. The inner coupling matrix $\Gamma = diag\{\gamma_1, \gamma_2, \ldots, \gamma_n\} \geq 0$ characterizes the connection of the jth state variable when $\gamma_j \neq 0$. The process noise $v_i(k) \in \mathbb{R}$, a Gaussian white noise sequence of zero mean, satisfies $\mathbb{E}{v_i}^2(k) \leq \theta_1^2$, with θ_1 being a positive scalar. The matrices A_i, B_i, and L_i are recognized as known real constant matrices. The outer-coupling configuration matrix $W = [w_{ij}] \in \mathbb{R}^{N\times N}$, indicative of the CNs topology, requires that $w_{ij} \geq 0$ $(i \neq j)$ but not uniformly zero. Generally, W is symmetric and ensures $\sum_{j=1}^{N} w_{ij} = \sum_{j=1}^{N} w_{ji} = 0$ for $i = 1, 2, \ldots, N$.

The nonlinear function $f(\cdot)$ is assumed to be continuous and satisfy the sector-bounded conditions as follows

$$[f(x) - f(y) - U_1(x-y)]^T \times [f(x) - f(y) - U_2(x-y)] \leq 0 \quad (2.2)$$

for all $x, y \in \mathbb{R}^n$, where U_1, U_2 are known constant matrices.

This paper aims to determine the states of (2.1) by leveraging measurements obtained from the network. It is crucial to acknowledge that in CNs, factors like limited resources and communication challenges often restrict the ability to gather data from all nodes. Consequently, our approach focuses on estimating the network's overall state using measurements derived from a select subset of nodes.

For the sake of generality, it is presupposed that access to the outputs of the initial q_0 nodes is available:

$$y_i(k) = C_i x_i(k), \quad 1 \leq i \leq q_0, \quad (2.3)$$

where $0 < q_0 < N$, $y_i(k) = [y_{i1}(k) \quad y_{i2}(k) \quad \cdots \quad y_{im}(k)]^T \in \mathbb{R}^m (1 \leq m \leq n)$ signifies the measurement output of the ith node, with $C_i \in \mathbb{R}^{m\times n}$ being a known constant matrix.

To optimize energy usage, we implement a DETM at each node. This mechanism decides the appropriate moments to transmit measurements to the state estimator. Specifically, for node i (where $1 \leq i \leq q_0$), the transmission times are designated as $0 \leq t_0^i \leq t_1^i \leq \cdots \leq t_l^i \leq \cdots$. These transmission times are determined on the basis of a predefined criterion:

$$t_{l+1}^i = min\Big\{k \in \mathbb{N} \mid k > t_l^i, \frac{1}{\delta_i}\rho_i(k) + \sigma_i y_i^T(k) y_i(k) - \xi_i^T(k)\xi_i(k) \leq 0\Big\}, \quad (2.4)$$

where δ_i and σ_i represent specified positive scalars, $\xi_i(k)$ is defined as $\xi_i(k) = y_i(k) - y_i(t_l^i)$, $y_i(t_l^i)$ represents the difference from the last transmitted measurement. Furthermore, $\rho_i(k)$ serves as an internal dynamical variable determined by

$$\rho_i(k+1) = \pi_i \rho_i(k) + \sigma_i y_i^T(k) y_i(k) - \xi_i^T(k)\xi_i(k), \quad (2.5)$$

where $0 < \pi_i < 1$ and $\rho_i(0) = \rho_0^i \geq 0$ is a specified initial condition.

With $\xi_i(k) = y_i(k) - y_i(t_l^i)$, the corresponding measurement output in the aforementioned scheme is depicted as

$$\bar{y}_i(k) = y_i(t_l^i). \quad (2.6)$$

It is important to note the data safety concerns stemming from the susceptibility of transmitted data to cyber threats. To effectively encapsulate the characteristics of these cyberattacks, the measurement that the estimator receives is modeled in the following manner.

$$\tilde{y}_i(k) = \alpha(k)(\bar{y}_i(k) + \beta(k)\vec{y}_i(k)), \quad 1 \le i \le q_0 \tag{2.7}$$

where $\vec{y}_i(k) = -\bar{y}_i(k) + \varpi(k)$ stands for the deceptive attack signal injected by the hostile attacker. Here, $\tilde{y}_i(k) \in \mathbb{R}^m$ is the measurement signal actually received from node i, $\varpi(k) \in \mathbb{R}^m$ is an error signal that satisfies

$$\mathbb{E}\left\{\varpi^T(k)\varpi(k)\right\} \le \theta_2^2, \tag{2.8}$$

with θ_2 being a given positive scalar. The variables $\alpha(k)$ and $\beta(k)$, both Bernoulli-distributed, are independently mutual and comply with these statistical characteristics:

$$\mathbb{E}\{\alpha(k)\} = Prob\{\alpha(k) = 1\} = \bar{\alpha},$$
$$\mathbb{E}\{\beta(k)\} = Prob\{\beta(k) = 1\} = \bar{\beta}.$$

From this, we have

$$\mathbb{E}\{\alpha(k) - \bar{\alpha}\} = 0, \quad \mathbb{E}\left\{(\alpha(k) - \bar{\alpha})^2\right\} = \bar{\alpha}(1 - \bar{\alpha}),$$
$$\mathbb{E}\left\{\beta(k) - \bar{\beta}\right\} = 0, \quad \mathbb{E}\left\{(\beta(k) - \bar{\beta})^2\right\} = \bar{\beta}(1 - \bar{\beta}),$$

where $\bar{\alpha}, \bar{\beta} \in [0, 1]$.

Remark 2.1. *This research focuses on the adversary's goal to impair estimation accuracy by targeting the transmitted measurement $\bar{y}_i(k)$. In the framework of model* (2.7)*, a scenario where $\alpha(k) = 0$ indicates a successful DoS attack, effectively halting all data transmission within the communication network. On the contrary, when $\alpha(k) = 1$ and $\beta(k) = 1$, the measurement output undergoes a deception attack, leading to the replacement of authentic data with a false signal. Notably, the condition $\alpha(k) = 1$ and $\beta(k) = 0$ signifies the secure transmission of measurement data to the estimator, free from cyberattacks. Both DoS and deception attacks may occur in varying patterns, either alternately or concurrently. Our numerical simulations consider scenarios where DoS attacks co-occur with deceptive tactics.*

Utilizing the measurements from q_0 nodes, the subsequent state estimators are constructed:

$$\begin{cases} \hat{x}_i(k+1) = A_i\hat{x}_i(k) + B_i\hat{x}_i(k-\tau(k)) + f(\hat{x}_i(k)) + \sum_{j=1}^{N} w_{ij}\Gamma\hat{x}_j(k) \\ \qquad + K_i\Big(\tilde{y}_i(k) - \alpha(k)C_i\hat{x}_i(k)\Big), i = 1, 2, \ldots, q_0, \\ \hat{x}_i(k+1) = A_i\hat{x}_i(k) + B_i\hat{x}_i(k-\tau(k)) + f(\hat{x}_i(k)) + \sum_{j=1}^{N} w_{ij}\Gamma\hat{x}_j(k) \\ \qquad i = q_0 + 1, q_0 + 2, \ldots, N, \end{cases} \tag{2.9}$$

where $\hat{x}_i(k)$ is the estimation of $x_i(k)$, and $K_i \in \mathbb{R}^{n\times m}$ ($i = 1, \ldots, q_0$) are the estimator gain parameters to be designed.

Define $e_i(k) = x_i(k) - \hat{x}_i(k)$ as the state estimation error, which is characterized by the following equation:

$$\begin{cases} e_i(k+1) = A_ie_i(k) + B_ie_i(k-\tau(k)) + \tilde{f}(e_i(k)) + \sum_{j=1}^{N} w_{ij}\Gamma e_j(k) \\ \qquad + L_iv_i(k) - K_i\Big(\tilde{y}_i(k) - \alpha(k)C_i\hat{x}_i(k)\Big), i = 1, 2, \ldots, q_0, \\ e_i(k+1) = A_ie_i(k) + B_ie_i(k-\tau(k)) + \tilde{f}(e_i(k)) + \sum_{j=1}^{N} w_{ij}\Gamma e_j(k) \\ \qquad + L_iv_i(k), i = q_0 + 1, q_0 + 2, \ldots, N, \end{cases} \tag{2.10}$$

where $\tilde{f}(e_i(k)) = f(x_i(k)) - f(\hat{x}_i(k))$.

To simplify the notation, it is further denoted

$$\aleph = \begin{bmatrix} \aleph_1^T & \aleph_2^T & \cdots & \aleph_N^T \end{bmatrix}^T,$$
$$(\aleph = x(k), x(k-\tau(k)), v(k), e(k), e(k-\tau(k))),$$
$$F(x(k)) = \begin{bmatrix} f^T(x_1(k)) & \cdots & f^T(x_N(k)) \end{bmatrix}^T,$$
$$R_1 = [I \quad I \quad \cdots \quad I]^T_{m\times q_0 m}, \bar{C} = [C \quad 0],$$
$$F(e(k)) = \begin{bmatrix} \tilde{f}^T(e_1(k)) & \cdots & \tilde{f}^T(e_N(k)) \end{bmatrix}^T,$$
$$\Im = diag\{\Im_1, \Im_2, \ldots, \Im_N\}(\Im = A, B, L),$$
$$Re = \begin{bmatrix} \Re_1^T \cdots \Re_{q_0}^T \end{bmatrix}^T (\Re = \xi(k), y(k)),$$
$$\lrcorner = diag\left\{\lrcorner_1, \lrcorner_2, \ldots, \lrcorner_{q_0}\right\}(\lrcorner = K, C), \quad \bar{K} = \begin{bmatrix} K^T & 0 \end{bmatrix}^T.$$

Subsequently, the dynamics of (2.10) is reformulated into the concise format

$$\begin{aligned} e(k+1) = &Ae(k) + Be(k-\tau(k)) + F(e(k)) + W \otimes \Gamma e(k) \\ &+ Lv(k) - \alpha(k)\bar{K}\bar{C}e(k) + \alpha(k)(1-\beta(k))\bar{K}\xi(k) \\ &+ \alpha(k)\beta(k)\bar{K}\bar{C}x(k) - \alpha(k)\beta(k)\bar{K}R_1\varpi(k). \end{aligned} \tag{2.11}$$

By defining $\eta(k) = \begin{bmatrix} x^T(k) & e^T(k) \end{bmatrix}^T$ and $F(\eta(k)) = \begin{bmatrix} F^T(x(k)) & F^T(e(k)) \end{bmatrix}^T$ we attain the following augmented system:

$$\begin{aligned}\eta(k+1) =& \mathcal{A}\eta(k) + \mathcal{B}\eta(k-\tau(k)) + F(\eta(k)) + \mathcal{L}v(k) \\ & - \alpha(k)C_1\eta(k) + \alpha(k)\beta(k)C_2\eta(k) \\ & + \alpha(k)(1-\beta(k))\mathcal{R}_2\xi(k) - \alpha(k)\beta(k)\mathcal{R}_1\varpi(k),\end{aligned} \tag{2.12}$$

where

$$\mathcal{A} = \begin{bmatrix} A + W \otimes \Gamma & 0 \\ 0 & A + W \otimes \Gamma \end{bmatrix}, \quad \mathcal{B} = \begin{bmatrix} B & 0 \\ 0 & B \end{bmatrix}$$
$$\mathcal{L} = \begin{bmatrix} L \\ L \end{bmatrix}, \quad C_1 = \begin{bmatrix} 0 & 0 \\ 0 & \bar{K}\bar{C} \end{bmatrix}, \quad C_2 = \begin{bmatrix} 0 & 0 \\ \bar{K}\bar{C} & 0 \end{bmatrix}$$
$$\mathcal{R}_1 = \begin{bmatrix} 0 \\ \bar{K}R_1 \end{bmatrix}, \quad \mathcal{R}_2 = \begin{bmatrix} 0 \\ \bar{K} \end{bmatrix}, \quad C = \begin{bmatrix} \bar{C} & 0 \end{bmatrix}.$$

In order to facilitate subsequent analysis, it is necessary to perform some required processing on (2.12). As a result, (2.12) can be reformulated as follows:

$$\begin{aligned}\eta(k+1) =& \Gamma_1 + (\alpha(k) - \bar{\alpha})\Gamma_2 + (\beta(k) - \bar{\beta})\Gamma_3 \\ & + (\alpha(k) - \bar{\alpha})(\beta(k) - \bar{\beta})\Gamma_4,\end{aligned} \tag{2.13}$$

where

$$\begin{aligned}\Gamma_1 =& \mathcal{A}\eta(k) + \mathcal{B}\eta(k-\tau(k)) + F(\eta(k)) + \mathcal{L}v(k) - \bar{\alpha}C_1\eta(k) \\ & + \bar{\alpha}\bar{\beta}C_2\eta(k) + \bar{\alpha}(1-\bar{\beta})\mathcal{R}_2\xi(k) - \bar{\alpha}\bar{\beta}\mathcal{R}_1\varpi(k), \\ \Gamma_2 =& -C_1\eta(k) + \bar{\beta}C_2\eta(k) + (1-\bar{\beta})\mathcal{R}_2\xi(k) - \bar{\beta}\mathcal{R}_1\varpi(k), \\ \Gamma_3 =& \bar{\alpha}C_2\eta(k) - \bar{\alpha}\mathcal{R}_2\xi(k) - \bar{\alpha}\mathcal{R}_1\varpi(k), \\ \Gamma_4 =& C_2\eta(k) - \mathcal{R}_2\xi(k) - \mathcal{R}_1\varpi(k).\end{aligned}$$

The ensuing definition is pivotal in the upcoming analysis and the design of the estimator.

Definition 2.1. *The evolution of the dynamics of the augmented estimation error according to* (2.12) *achieves the EMSUB status if there are positive scalars $d, \bar{\gamma}$, and $\mu \in [0, 1)$ such that*

$$\mathbb{E}\left\{\|\eta(k)\|^2\right\} \leq d\mu^k + \gamma(k), \quad \lim_{k\to+\infty} \gamma(k) = \bar{\gamma}.$$

3. Main results

This section delves into the state estimation challenge for CN (2.1), focusing specifically on data from a subset of network nodes. Initially, we present an essential lemma for subsequent derivations.

Lemma 3.1. *For the DETM* (2.4)-(2.5) *with $\rho_0^i \geq 0$ ($1 \leq i \leq q_0$), the internal dynamic variable satisfies $\rho_i(k) \geq 0$ for all $k \geq 0$ if the parameters π_i ($0 < \pi_i < 1$) and δ_i ($\delta_i > 0$) satisfy $\pi_i\delta_i \geq 1$.*

Proof. For all $k \geq 0$, according to the triggering condition (2.4), it follows that

$$\frac{1}{\delta_i}\rho_i(k) + \sigma_i y_i^T(k)y_i(k) - \xi_i^T(k)\xi_i(k) \geq 0.$$

Subsequently, by virtue of Eq (2.5), one deduces that

$$\rho_i(k+1) \geq (\pi_i - \frac{1}{\delta_i})\rho_i(k) \geq \cdots \geq (\pi_i - \frac{1}{\delta_i})^{k+1}\rho_0^i,$$

which leads to the clear observation that $\rho(k) \geq 0$ for all $k \geq 0$ given the prerequisites $\pi_i\delta_i \geq 1$ and $\rho_0^i \geq 0$. Hence, the proof is concluded. □

Theorem 3.1. *For all $i = 1, 2, \ldots, q_0$, assume that Lemma 3.1 is satisfied. Given the estimator parameters K_i and the positive constants θ_1, θ_2. The augmented estimation error dynamics, as indicated in* (2.12)*, achieves EMSUB status provided there are matrices $P = diag\{P_1, P_2\} > 0$ ($P_1 = diag\{P_{11}, P_{12}, \ldots, P_{1N}\}$, $P_2 = diag\{P_{21}, P_{22}, \ldots, P_{2N}\}$), $Q > 0$, and positive scalars λ_1, λ_2, λ_3, λ_4 satisfying*

$$\Xi = \begin{bmatrix} \Psi & * \\ \bar{P}\bar{\Xi} & -\bar{P} \end{bmatrix} < 0, \tag{3.1}$$

where $\bar{P} = diag\{P, P, P, P\}$,

$$\Psi = \begin{bmatrix} \Psi_{11} & \lambda_3(I \otimes \tilde{U}_2) & 0 & 0 & 0 & 0 & 0 \\ * & -\lambda_3 I & 0 & 0 & 0 & 0 & 0 \\ * & * & -Q & 0 & 0 & 0 & 0 \\ * & * & * & -\lambda_1 I & 0 & 0 & 0 \\ * & * & * & * & -\lambda_2 I & 0 & 0 \\ * & * & * & * & * & -\Psi_{66} & 0 \\ * & * & * & * & * & * & \Psi_{77} \end{bmatrix},$$

$$\bar{\Xi} = \begin{bmatrix} \Xi_1{}^T & \chi_\alpha^2\Xi_2^T & \chi_\beta^2\Xi_3^T & \chi_\alpha^2\chi_\beta^2\Xi_4^T \end{bmatrix}^T,$$
$$\Xi_1 = \begin{bmatrix} \Xi_{11} & I & \mathcal{B} & \mathcal{L} & -\bar{\alpha}\bar{\beta}\mathcal{R}_1 & \bar{\alpha}(1-\bar{\beta})\mathcal{R}_2 & 0 \end{bmatrix},$$
$$\Xi_2 = \begin{bmatrix} -C_1+\bar{\beta}C_2 & 0 & 0 & 0 & -\bar{\beta}\mathcal{R}_1 & (1-\bar{\beta})\mathcal{R}_2 & 0 \end{bmatrix},$$
$$\tilde{U}_1 = \frac{U_1^TU_2 + U_2^TU_1}{2}, \tilde{U}_2 = \frac{U_1^T + U_2^T}{2},$$
$$\Xi_3 = \begin{bmatrix} \bar{\alpha}C_2 & 0 & 0 & 0 & -\bar{\alpha}\mathcal{R}_1 & -\bar{\alpha}\mathcal{R}_2 & 0 \end{bmatrix},$$
$$\Xi_4 = \begin{bmatrix} C_2 & 0 & 0 & 0 & -\mathcal{R}_1 & -\mathcal{R}_2 & 0 \end{bmatrix},$$
$$\Psi_{77} = diag\left\{\frac{\pi_1 - 1 + \lambda_4}{\delta_1}, \ldots, \frac{\pi_{q_0} - 1 + \lambda_4}{\delta_{q_0}}\right\}$$
$$\Psi_{66} = diag\left\{\left(\frac{1}{\delta_1} + \lambda_4\right)I, \ldots, \left(\frac{1}{\delta_{q_0}} + \lambda_4\right)I\right\},$$
$$\Xi_{11} = \mathcal{A} - \bar{\alpha}C_1 + \bar{\alpha}\bar{\beta}C_2, \theta^2 = \lambda_1 N\theta_1^2 + \lambda_2\theta_2^2,$$
$$\Psi_{11} = -P + (\tau_2 - \tau_1 + 1)Q + \Phi C^TC - \lambda_3(I \otimes \tilde{U}_1),$$
$$\Phi = diag\left\{\left(\lambda_4\sigma_1 + \frac{\sigma_1}{\delta_1}\right)I, \ldots, \left(\lambda_4\sigma_{q_0} + \frac{\sigma_{q_0}}{\delta_{q_0}}\right)I\right\}.$$

Proof. We select the following Lyapunov functional candidate:

$$M(k) = V(k) + \rho(k), \tag{3.2}$$

where

$$V(k) = \sum_{i=1}^{3} V_i(k), \quad \rho(k) = \sum_{i=1}^{q_0} \frac{1}{\delta_i}\rho_i(k),$$

with $V_1(k) = \eta^T(k)P\eta(k)$, $V_2(k) = \sum\limits_{i=k-\tau(k)}^{k-1} \eta^T(i)Q\eta(i)$, $V_3(k) = \sum\limits_{j=k-\tau_2+1}^{k-\tau_1}\sum\limits_{i=j}^{k-1} \eta^T(i)Q\eta(i)$. According to system (2.13), the mathematical expectations of the variation in $V(k)$ and $\rho(k)$ are calculated as

$$\begin{aligned}\mathbb{E}\{\Delta V_1(k)\} =& \mathbb{E}\{V_1(k+1) - V_1(k)\}\\ =& \Gamma_1^TP\Gamma_1 + \chi_\alpha^2\Gamma_2^TP\Gamma_2 + \chi_\beta^2\Gamma_3^TP\Gamma_3\\ &+ \chi_\alpha^2\chi_\beta^2\Gamma_4^TP\Gamma_4 - \eta^T(k)P\eta(k),\end{aligned} \tag{3.3}$$

where $\chi_\alpha^2 = \bar{\alpha}(1-\bar{\alpha}), \chi_\beta^2 = \bar{\beta}(1-\bar{\beta})$.

$$\begin{aligned}\mathbb{E}\{\Delta V_2(k)\} =& \eta^T(k)Q\eta(k) - \eta^T(k-\tau(k))Q\eta(k-\tau(k))\\ &+ \sum_{i=k-\tau(k+1)+1}^{k-\tau_1} \eta^T(i)Q\eta(i) + \sum_{i=k-\tau_1+1}^{k-1} \eta^T(i)Q\eta(i)\\ &- \sum_{i=k-\tau(k)+1}^{k-1} \eta^T(i)Q\eta(i)\\ \le& \eta^T(k)Q\eta(k) - \eta^T(k-\tau(k))Q\eta(k-\tau(k))\\ &+ \sum_{i=k-\tau_2+1}^{k-\tau_1} \eta^T(i)Q\eta(i).\end{aligned} \tag{3.4}$$

$$\mathbb{E}\{\Delta V_3(k)\} = (\tau_2 - \tau_1)\eta^T(k)Q\eta(k) - \sum_{i=k-\tau_2+1}^{k-\tau_1} \eta^T(i)Q\eta(i) \tag{3.5}$$

and

$$\begin{aligned}\mathbb{E}\{\Delta\rho(k)\} =& \sum_{i=1}^{q_0} \frac{1}{\delta_i}\Big(\rho_i(k+1) - \rho_i(k)\Big)\\ =& \sum_{i=1}^{q_0} \frac{1}{\delta_i}\Big[(\pi_i - 1)\rho_i(k) + \sigma_i y_i^T(k)y_i(k) - \xi_i^T(k)\xi_i(k)\Big]\\ =& \sum_{i=1}^{q_0} \frac{\pi_i - 1}{\delta_i}\rho_i(k) + \sum_{i=1}^{q_0} \frac{\sigma_i}{\delta_i}y_i^T(k)y_i(k)\\ &- \sum_{i=1}^{q_0} \frac{1}{\delta_i}\xi_i^T(k)\xi_i(k).\end{aligned} \tag{3.6}$$

On the other hand, by considering $\mathbb{E}\{v_i^2(k)\} \le \theta_1^2$, one obtains

$$\mathbb{E}\left\{v^T(k)v(k)\right\} \le N\theta_1^2. \tag{3.7}$$

Taking into account the non-linearity (2.2), one has

$$\Lambda = \begin{bmatrix} \eta(k) \\ F(\eta(k)) \end{bmatrix}^T \begin{bmatrix} I \otimes \tilde{U}_1 & I \otimes (-\tilde{U}_2) \\ * & I \end{bmatrix} \begin{bmatrix} \eta(k) \\ F(\eta(k)) \end{bmatrix} \le 0. \tag{3.8}$$

Based on the triggering condition (2.4), we derive

$$\sum_{i=1}^{q_0} \frac{1}{\delta_i}\rho_i(k) + \sum_{i=1}^{q_0} \sigma_i y_i^T(k)y_i(k) - \sum_{i=1}^{q_0} \xi_i^T(k)\xi_i(k) \ge 0. \tag{3.9}$$

Additionally, it follows from (3.3)–(3.5) that

$$\begin{aligned}\mathbb{E}\{\Delta V(k)\} \le& \Gamma_1^TP\Gamma_1 + \chi_\alpha^2\Gamma_2^TP\Gamma_2 + \chi_\beta^2\Gamma_2^TP\Gamma_2 + \chi_\alpha^2\chi_\beta^2\Gamma_3^TP\Gamma_3\\ &- \eta^T(k)P\eta(k) - \eta^T(k-\tau(k))Q\eta(k-\tau(k))\\ &+ (\tau_2 - \tau_1 + 1)\eta^T(k)Q\eta(k)\\ \le& \bar{\eta}^T(k)\Big(\bar{\Xi}^T\bar{P}\bar{\Xi}\Big)\bar{\eta}(k) + (\tau_2 - \tau_1 + 1)\eta^T(k)Q\eta(k)\\ &- \eta^T(k)P\eta(k) - \eta^T(k-\tau(k))Q\eta(k-\tau(k)),\end{aligned} \tag{3.10}$$

where $\bar{\rho}(k) = \left[\rho_1^{\frac{1}{2}}(k) \;\; \rho_2^{\frac{1}{2}}(k) \;\; \cdots \;\; \rho_{q_0}^{\frac{1}{2}}(k)\right]^T$, $\bar{\eta}(k) = \left[\eta^T(k),\ F^T(\eta(k)),\ \eta^T(k-\tau(k)),\ v^T(k),\ \varpi^T(k),\ \xi^T(k),\ \bar{\rho}(k)\right]^T$.

By taking (2.8) and (3.7)–(3.9) into account, it is deduced from (3.6) and (3.10) that

$$\begin{aligned}\mathbb{E}\{\Delta M(k)\} &= \mathbb{E}\{\Delta V(k)\} + \mathbb{E}\{\Delta\rho(k)\}\\ &\le \bar{\eta}^T(k)\Big(\bar{\Xi}^T\bar{P}\bar{\Xi} + \Psi\Big)\bar{\eta}(k) + \theta^2. \end{aligned} \tag{3.11}$$

Utilizing the Schur complement lemma on (3.1) yields

$$\bar{\Xi}^T\bar{P}\bar{\Xi} + \Psi < 0.$$

From this, we can further deduce:

$$\mathbb{E}\{\Delta M(k)\} \le a\mathbb{E}\left\{\|\varphi(k)\|^2\right\} + \theta^2, \tag{3.12}$$

where $\varphi(k) = \begin{bmatrix}\eta^T(k) & \bar{\rho}^T(k)\end{bmatrix}^T$ and $a = \lambda_{max}\Big(\bar{\Xi}^T\bar{P}\bar{\Xi} + \Psi\Big)$.

Due to the definition of $M(k)$, we conclude that

$$\begin{aligned}\mathbb{E}\Big\{M(k)\Big\} \le&(\tau_2 - \tau_1 + 1)\lambda_{max}(Q)\sum_{i=k-\tau_2}^{k-1}\mathbb{E}\left\{\|\eta(i)\|^2\right\}\\ &+ \lambda_{max}(P)\mathbb{E}\left\{\|\eta(k)\|^2\right\} + \sum_{i=1}^{q_0}\frac{1}{\delta_i}\rho_i(k)\\ \le&(\tau_2 - \tau_1 + 1)\lambda_{max}(Q)\sum_{i=k-\tau_2}^{k-1}\mathbb{E}\left\{\|\varphi(i)\|^2\right\}\\ &+ b\mathbb{E}\left\{\|\varphi(k)\|^2\right\}, \end{aligned} \tag{3.13}$$

where $b = max\Big\{\lambda_{max}(P), (1/\delta_1), \ldots, (1/\delta_{q_0})\Big\}$.

For a given scalar $c > 1$, the aforementioned inequality (3.13) implies that

$$\begin{aligned}&\mathbb{E}\left\{c^{k+1}M(k+1)\right\} - \mathbb{E}\left\{c^kM(k)\right\}\\ =&c^{k+1}\mathbb{E}\Big\{M(k+1) - M(k)\Big\} + c^k(c-1)\mathbb{E}\Big\{M(k)\Big\}\\ \le&c^k\psi(c)\mathbb{E}\left\{\|\varphi(k)\|^2\right\} + c^k\varrho(c)\sum_{i=k-\tau_2}^{k-1}\mathbb{E}\left\{\|\varphi(i)\|^2\right\} + c^{k+1}\theta^2, \end{aligned} \tag{3.14}$$

where $\psi(c) = ca + (c-1)b$, $\varrho(c) = (c-1)(\tau_2 - \tau_1 + 1)\lambda_{max}(Q)$.

Assuming $r \ge \tau_2 + 1$ is a positive integer and summing both sides of (3.14) from 0 to $r-1$ with respect to k, it results in

$$\begin{aligned}\mathbb{E}\Big\{c^rM(r)\Big\} - \mathbb{E}\Big\{M(0)\Big\} \le&\psi(c)\sum_{k=0}^{r-1}c^k\mathbb{E}\left\{\|\varphi(k)\|^2\right\} + \frac{c(1-c^r)}{1-c}\theta^2\\ &+ \varrho(c)\sum_{k=0}^{r-1}\sum_{i=k-\tau_2}^{k-1}c^k\mathbb{E}\left\{\|\varphi(i)\|^2\right\}, \end{aligned} \tag{3.15}$$

where $\varrho(c)\sum_{k=0}^{r-1}\sum_{i=k-\tau_2}^{k-1}c^k\mathbb{E}\left\{\|\varphi(i)\|^2\right\}$ can be computed as follows:

$$\begin{aligned}&\varrho(c)\sum_{k=0}^{r-1}\sum_{i=k-\tau_2}^{k-1}c^k\mathbb{E}\left\{\|\varphi(i)\|^2\right\}\\ \le&\varrho(c)\left(\sum_{i=-\tau_2}^{-1}\sum_{k=0}^{i+\tau_2} + \sum_{i=0}^{r-1-\tau_2}\sum_{k=i+1}^{i+\tau_2} + \sum_{i=r-\tau_2}^{r-1}\sum_{k=i+1}^{r-1}\right)c^k\mathbb{E}\left\{\|\varphi(i)\|^2\right\}\\ \le&\varrho(c)\tau_2\sum_{i=-\tau_2}^{-1}c^{i+\tau_2}\mathbb{E}\left\{\|\varphi(i)\|^2\right\} + \varrho(c)\tau_2\sum_{i=0}^{r-1-\tau_2}c^{i+\tau_2}\mathbb{E}\left\{\|\varphi(i)\|^2\right\}\\ &+ \varrho(c)\tau_2\sum_{i=r-\tau_2}^{r-1}c^{i+\tau_2}\mathbb{E}\left\{\|\varphi(i)\|^2\right\}\\ \le&\varrho(c)\frac{\tau_2c^{\tau_2}}{c-1}\max_{-\tau_2\le i\le 0}\mathbb{E}\left\{\|\varphi(i)\|^2\right\} + \varrho(c)\tau_2c^{\tau_2}\sum_{i=0}^{r-1}c^i\mathbb{E}\left\{\|\varphi(i)\|^2\right\}. \end{aligned} \tag{3.16}$$

Then, it is obtained that

$$\begin{aligned}&\mathbb{E}\Big\{c^rM(r)\Big\} - \mathbb{E}\Big\{M(0)\Big\}\\ \le&\psi(c)\sum_{k=0}^{r-1}c^k\mathbb{E}\left\{\|\varphi(k)\|^2\right\} + \tau_2c^{\tau_2}\varrho(c)\sum_{i=0}^{r-1}c^i\mathbb{E}\left\{\|\varphi(i)\|^2\right\}\\ &+ \frac{\tau_2c^{\tau_2}\varrho(c)}{c-1}\max_{-\tau_2\le i\le 0}\mathbb{E}\left\{\|\varphi(i)\|^2\right\} + \frac{c(1-c^r)}{1-c}\theta^2\\ =&\frac{\tau_2c^{\tau_2}\varrho(c)}{c-1}\max_{-\tau_2\le i\le 0}\mathbb{E}\left\{\|\varphi(i)\|^2\right\} + \frac{c(1-c^r)}{1-c}\theta^2\\ &+ \epsilon(c)\sum_{k=0}^{r-1}c^k\mathbb{E}\left\{\|\varphi(k)\|^2\right\}, \end{aligned} \tag{3.17}$$

where $\epsilon(c) = \psi(c) + \tau_2c^{\tau_2}\varrho(c)$.

Since $\epsilon(1) = a < 0$ and $\epsilon(+\infty) = +\infty$, we can find a scalar $c_0 > 1$ such that $\epsilon(c_0) = 0$. Therefore, we have

$$\begin{aligned}&\mathbb{E}\Big\{c^rM(r)\Big\} - \mathbb{E}\Big\{M(0)\Big\}\\ \le&\frac{\tau_2c_0^{\tau_2}\varrho(c_0)}{c_0-1}\max_{-\tau_2\le i\le 0}\mathbb{E}\left\{\|\varphi(i)\|^2\right\} + \frac{c_0(1-c_0^r)}{1-c_0}\theta^2. \end{aligned} \tag{3.18}$$

From (3.13), it is obvious that

$$\mathbb{E}\Big\{M(0)\Big\} \le \varsigma\tau_2\max_{-\tau_2\le i\le 0}\mathbb{E}\left\{\|\varphi(i)\|^2\right\}, \tag{3.19}$$

in which $\varsigma = max\{b, (\tau_2 - \tau_1 + 1)\lambda_{max}(Q)\}$. Furthermore, according to the definition of $M(k)$, one derives

$$\mathbb{E}\Big\{M(r)\Big\} \ge u\mathbb{E}\left\{\|\varphi(r)\|^2\right\}, \tag{3.20}$$

with $u = min\left\{\lambda_{min}(P), (1/\delta_1), \ldots, (1/\delta_{q_0})\right\}$.

By substituting (3.19) and (3.20) into (3.18), one has

$$\mathbb{E}\left\{\|\varphi(r)\|^2\right\} \leq \frac{\phi(c_0)}{uc_0^r} + \frac{c_0^r - 1}{uc_0^{r-1}(c_0-1)}\theta^2, \tag{3.21}$$

with $\phi(c_0) = \left(\varsigma\tau_2 + \frac{\tau_2 c_0^{\tau_2}\varrho(c_0)}{c_0-1}\right)\max_{-\tau_2\leq i\leq 0}\mathbb{E}\left\{\|\varphi(i)\|^2\right\}$.

Consequently, we obtain the final result

$$\mathbb{E}\left\{\|\eta(k)\|^2\right\} \leq \mathbb{E}\left\{\|\varphi(r)\|^2\right\} \leq \frac{\phi(c_0)}{uc_0^r} + \frac{(c_0^r-1)\theta^2}{uc_0^{r-1}(c_0-1)}. \tag{3.22}$$

According to Definition 2.1, the augmented system (2.12) is said to be EMSUB by setting $d = (\phi(c_0)/u)$, $\mu = (1/c_0)$ and $\gamma(r) = (c_0^r - 1)\theta^2/uc_0^{r-1}(c_0-1)$. Moreover, the ultimate bound is derived as

$$\bar{\gamma} = \lim_{r\to+\infty}\gamma(r) = \frac{c_0\theta^2}{u(c_0-1)},$$

with $c_0 > 1$ satisfying $\psi(c_0) + \tau_M c_0^{\tau_2}\varrho(c_0) = 0$. Thus, the proof of this theorem is concluded. □

Theorem 3.2. *Let Lemma 3.1 be satisfied and positive constants θ_1, θ_2 be given. The augmented estimation error dynamics* (2.12) *is EMSUB if there exist matrices $P > 0$, $Q > 0$, real-valued matrices $\bar{X} = \begin{bmatrix} X^T & 0 \end{bmatrix}^T$ ($X = diag\left\{X_1, X_2, \ldots, X_{q_0}\right\}$), and positive scalars λ_1, λ_2, λ_3, λ_4 such that*

$$\Pi = \begin{bmatrix} \Psi & * \\ \tilde{\Xi} & -\bar{P}, \end{bmatrix} < 0 \tag{3.23}$$

in which P has the same structure as that of Theorem 3.1, $\tilde{\Xi}^T = \left[\tilde{\Xi}_1^T, \chi_\alpha^2\tilde{\Xi}_2{}^T, \chi_\beta^2\tilde{\Xi}_3{}^T, \chi_\alpha^2\chi_\beta^2\tilde{\Xi}_4^T\right]$,

$$\tilde{\mathcal{L}} = \begin{bmatrix} PL \\ PL \end{bmatrix}, \quad \tilde{\mathcal{B}} = \begin{bmatrix} PB & 0 \\ 0 & PB \end{bmatrix}, \quad \tilde{C}_1 = \begin{bmatrix} 0 & 0 \\ \bar{X}\bar{C} & 0 \end{bmatrix},$$

$$\tilde{\Xi}_1 = \begin{bmatrix} \tilde{\Xi}_{11} & P & \tilde{\mathcal{B}} & \tilde{\mathcal{L}} & -\bar{\alpha}\bar{\beta}\tilde{\mathcal{R}}_1 & \bar{\alpha}(1-\bar{\beta})\tilde{\mathcal{R}}_2 & 0 \end{bmatrix},$$

$$\tilde{C}_2 = \begin{bmatrix} 0 & 0 \\ \bar{X}\bar{C} & 0 \end{bmatrix}\tilde{\Xi}_{11} = \tilde{\mathcal{A}} - \bar{\alpha}\tilde{C}_1 + \bar{\alpha}\bar{\beta}\tilde{C}_2,$$

$$\tilde{\Xi}_2 = \begin{bmatrix} -\tilde{C}_1 + \bar{\beta}\tilde{C}_2 & 0 & 0 & 0 & -\bar{\beta}\tilde{\mathcal{R}}_1 & (1-\bar{\beta})\tilde{\mathcal{R}}_2 & 0 \end{bmatrix},$$

$$\tilde{\Xi}_3 = \begin{bmatrix} \bar{\alpha}\tilde{C}_2 & 0 & 0 & 0 & -\bar{\alpha}\tilde{\mathcal{R}}_1 & -\bar{\alpha}\tilde{\mathcal{R}}_2 & 0 \end{bmatrix},$$

$$\tilde{\Xi}_4 = \begin{bmatrix} \tilde{C}_2 & 0 & 0 & 0 & -\tilde{\mathcal{R}}_1 & -\tilde{\mathcal{R}}_2 & 0 \end{bmatrix},$$

$$\tilde{\mathcal{A}} = \begin{bmatrix} PA + PW\otimes\Gamma & 0 \\ 0 & PA + PW\otimes\Gamma \end{bmatrix},$$

$$\tilde{\mathcal{R}}_1 = \begin{bmatrix} 0 \\ \bar{X}R_1 \end{bmatrix}, \quad \tilde{\mathcal{R}}_2 = \begin{bmatrix} 0 \\ \bar{X} \end{bmatrix},$$

and Ψ is defined in (3.1). *Additionally, the estimator gain matrix can be obtained by:*

$$K_i = P_{2i}^{-1}X_i, \quad (i = 1, 2, \ldots, q_0). \tag{3.24}$$

Proof. Letting $\bar{X} = P_2\bar{K}$, the substantiation of Theorem 3.2 is directly derived from the proof of Theorem 3.1. □

It is worth noting that when we take $\delta_i \to +\infty$, the proposed DETM encompasses the static one as follows:

$$t_{l+1}^i = min\left\{k \in \mathbb{N} \mid k > t_l^i, \sigma_i y_i^T(k)y_i(k) - \xi_i^T(k)\xi_i(k) < 0\right\}, \tag{3.25}$$

for all $i = 1, 2, \ldots, q_0$. As such, the corresponding results for the SETM can be easily derived from Theorem 3.2.

Corollary 3.1. *Let the positive constants θ_1, θ_2 be given. The augmented estimation error dynamics* (2.12) *is EMSUB under the SETM* (3.25) *if there exist matrices $\tilde{P} > 0$, $\tilde{Q} > 0$, real-valued matrices $\tilde{X} = \begin{bmatrix} \check{X}^T & 0 \end{bmatrix}^T$ ($\check{X} = diag\left\{(\check{X}_1, \check{X}_2, \ldots, \check{X}_{q_0}\right\}$) and positive scalars $\tilde{\lambda}_1$, $\tilde{\lambda}_2$, $\tilde{\lambda}_3$, $\tilde{\lambda}_4$ that meet the subsequent inequality:*

$$\Upsilon = \begin{bmatrix} \Theta & * \\ \vec{P}\vec{\Upsilon} & -\vec{P} \end{bmatrix} < 0, \tag{3.26}$$

where $\bar{\Upsilon}^T = \left[\Upsilon_1{}^T, \chi_\alpha^2\Upsilon_2{}^T, \chi_\beta^2\Upsilon_3{}^T, \chi_\alpha^2\chi_\beta^2\Upsilon_4{}^T\right]$,

$$\Theta = \begin{bmatrix} \Theta_{11} & \tilde{\lambda}_3(I\otimes\tilde{U}_2) & 0 & 0 & 0 & 0 \\ * & -\tilde{\lambda}_3 I & 0 & 0 & 0 & 0 \\ * & * & -\tilde{Q} & 0 & 0 & 0 \\ * & * & * & -\tilde{\lambda}_1 I & 0 & 0 \\ * & * & * & * & -\tilde{\lambda}_2 I & 0 \\ * & * & * & * & * & -\Theta_{66} \end{bmatrix},$$

$$\Theta_{11} = -\tilde{P} + (\tau_2 - \tau_1 + 1)\tilde{Q} + \tilde{\Phi}C^TC - \tilde{\lambda}_3(I\otimes\tilde{U}_1),$$

$$\vec{P} = diag\left\{\tilde{P}, \tilde{P}, \tilde{P}, \tilde{P}\right\}\tilde{\Phi} = diag\left\{\tilde{\lambda}_4\sigma_1 I, \ldots, \tilde{\lambda}_4\sigma_{q_0}I\right\},$$

$$\Theta_{66} = diag\left\{\tilde{\lambda}_4 I, \ldots, \tilde{\lambda}_4 I\right\}, \quad \tilde{\theta}^2 = \tilde{\lambda}_1 N\theta_1^2 + \tilde{\lambda}_2\theta_2^2,$$

$$\vec{\mathcal{L}} = \begin{bmatrix} \tilde{P}L \\ \tilde{P}L \end{bmatrix}, \quad \vec{\mathcal{B}} = \begin{bmatrix} \tilde{P}B & 0 \\ 0 & \tilde{P}B \end{bmatrix},$$

$$\vec{\mathcal{R}}_1 = \begin{bmatrix} 0 \\ \tilde{X}R_1 \end{bmatrix}, \quad \vec{\mathcal{R}}_2 = \begin{bmatrix} 0 \\ \tilde{X} \end{bmatrix},$$

$$\Upsilon_1 = \begin{bmatrix} \Upsilon_{11} & \tilde{P} & \vec{\mathcal{B}} & \vec{\mathcal{L}} & -\bar{\alpha}\bar{\beta}\vec{\mathcal{R}}_1 & \bar{\alpha}(1-\bar{\beta})\vec{\mathcal{R}}_2 \end{bmatrix},$$

$$\Upsilon_{11} = \vec{\mathcal{A}} - \bar{\alpha}\vec{C}_1 + \bar{\alpha}\bar{\beta}\vec{C}_2,$$

$$\Upsilon_2 = \begin{bmatrix} -\vec{C}_1 + \bar{\beta}\vec{C}_2 & 0 & 0 & 0 & -\bar{\beta}\vec{\mathcal{R}}_1 & (1-\bar{\beta})\vec{\mathcal{R}}_2 \end{bmatrix},$$

$$\Upsilon_3 = \begin{bmatrix} \bar{\alpha}\vec{C}_2 & 0 & 0 & 0 & -\bar{\alpha}\vec{\mathcal{R}}_1 & -\bar{\alpha}\vec{\mathcal{R}}_2 \end{bmatrix},$$
$$\Upsilon_4 = \begin{bmatrix} \vec{C}_2 & 0 & 0 & 0 & -\vec{\mathcal{R}}_1 & -\vec{\mathcal{R}}_2 \end{bmatrix},$$
$$\vec{C}_2 = \begin{bmatrix} 0 & 0 \\ \tilde{X}\bar{C} & 0 \end{bmatrix}, \quad \vec{C}_1 = \begin{bmatrix} 0 & 0 \\ 0 & \tilde{X}\bar{C} \end{bmatrix},$$
$$\vec{\mathcal{A}} = \begin{bmatrix} \tilde{P}A + \tilde{P}W \otimes \Gamma & 0 \\ 0 & \tilde{P}A + \tilde{P}W \otimes \Gamma \end{bmatrix}.$$

If the inequality (3.26) *is attainable, the desired estimator parameters can be represented by*

$$K_i = \tilde{P}_{2i}^{-1}\check{X}_i, \quad (i = 1, 2, \ldots, q_0), \tag{3.27}$$

which guarantees that the augmented estimation error dynamics (2.12) *achieves EMSUB, with the ultimate bound described as follows*

$$\bar{\gamma} = \frac{\tilde{c}_0\tilde{\theta}^2}{\tilde{u}(\tilde{c}_0 - 1)},$$

where $\tilde{u} = \lambda_{min}(\tilde{P})$ *and* $\tilde{c}_0 > 1$ *satisfies*

$$\tilde{\psi}(\tilde{c}_0) + \tau_2\tilde{c}_0^{\tau_2}\tilde{\varrho}(\tilde{c}_0) = 0$$

with

$$\tilde{a} = \lambda_{max}\Big(\bar{\Upsilon}^T\vec{P}\bar{\Upsilon} + \Theta\Big), \quad \tilde{b} = \lambda_{max}(\tilde{P}),$$
$$\tilde{\psi}(\tilde{c}) = \tilde{c}\tilde{a} + (c-1)\tilde{b}, \quad \tilde{\varrho}(\tilde{c}) = (\tilde{c}-1)(\tau_2 - \tau_1 + 1)\lambda_{max}(\tilde{Q}).$$

Proof. The proof of this corollary can be directly deduced from Theorem 3.1 upon letting $\delta_i \to +\infty$ $(i = 1, 2, \ldots, q_0)$. □

Remark 3.1. *The DETC-based PNBSE issue has been addressed for CNs under hybrid cyberattacks. This theorem distinguishes itself from existing research results in the following three aspects:*

(1) By considering hybrid attacks including both DoS and deception forms, the state estimator is designed to make the error dynamics adhere to EMSUB in the sense of security requirements.

(2) An DETM with dynamical variable is introduced for effectively reducing the data transmission from sensors to estimator while guaranteeing the estimation performance.

(3) It pioneers a technique for state estimation in CNs that relies on acquiring measurements from a selective group of nodes, optimizing both resource allocation and data accuracy.

4. A numerical example

In this section, a numerical example is provided to illustrate the efficacy of the state estimation approach developed in this research.

Considering a CN with four nodes described in (2.1), we focus on accessing measurements from only the first two nodes. The network parameters are chosen as below:

$$A_1 = A_2 = \begin{bmatrix} -0.02 & -0.05 & -0.04 \\ 0.06 & 0.05 & -0.02 \\ 0.01 & 0.02 & -0.03 \end{bmatrix},$$
$$A_3 = A_4 = \begin{bmatrix} -0.01 & -0.03 & -0.02 \\ 0.03 & 0.02 & -0.02 \\ 0.04 & 0.01 & -0.02 \end{bmatrix},$$
$$B_1 = B_2 = \begin{bmatrix} 0.01 & 0.02 & 0.01 \\ 0.01 & -0.01 & 0.01 \\ 0.02 & 0.01 & 0.02 \end{bmatrix},$$
$$B_3 = B_4 = \begin{bmatrix} 0.02 & 0.01 & 0.02 \\ 0.03 & -0.01 & 0.01 \\ 0.02 & 0.03 & 0.02 \end{bmatrix},$$
$$L_1 = L_2 = \begin{bmatrix} 0.02 \\ 0.01 \\ 0.1 \end{bmatrix}, \quad L_3 = L_4 = \begin{bmatrix} 0.01 \\ 0.03 \\ 0.01 \end{bmatrix},$$
$$C_1 = C_2 = \begin{bmatrix} 0.2 & 0.2 & 0.2 \\ 0.1 & 0.1 & 0.2 \end{bmatrix},$$
$$W = \begin{bmatrix} -0.05 & 0.02 & 0.02 & 0.01 \\ 0.02 & -0.05 & 0.02 & 0.01 \\ 0.02 & 0.02 & -0.06 & 0.02 \\ 0.01 & 0.01 & 0.02 & -0.04 \end{bmatrix},$$
$$\Gamma = 0.55I, \tau(k) = 2 + \frac{1 + (-1)^k}{2}, \tau_1 = 2, \tau_2 = 3,$$
$$\sigma_1 = 0.4, \sigma_2 = 0.5, \theta_1 = 0.2, \theta_2 = 0.3,$$
$$\delta_1 = \delta_2 = 12, \bar{\alpha} = 0.4, \bar{\beta} = 0.2, \pi_1 = 0.7, \pi_2 = 0.5.$$

The nonlinear vector-valued functions $f(x_i(k))$ $(i = 1, 2, 3, 4)$ are selected to be

$$f(x_i(k)) = \left[f_1(x_i(k)), f_2(x_i(k)), f_3(x_i(k))\right]^T,$$

wherein

$$
\begin{aligned}
f_1(x_i(k)) &= -0.1x_{i1}(k) \\
&\quad + 0.1(|x_{i1}(k)+2| - |x_{i1}(k)-2|) + 0.1x_{i2}(k), \\
f_2(x_i(k)) &= tanh(-0.2x_{i2}(k)), \\
f_3(x_i(k)) &= tanh(-0.2x_{i3}(k)),
\end{aligned}
$$

$x_{ir}(k)(r = 1,2,3)$ denotes the r-th component of $x_i(k)$. Consequently, it is readily obtained that

$$
U_1 = \begin{bmatrix} 0.1 & 0.1 & 0 \\ 0 & -0.2 & 0 \\ 0 & 0 & -0.2 \end{bmatrix}, \quad U_2 = \begin{bmatrix} -0.1 & 0.1 & 0 \\ 0 & 0 & 0 \\ 0 & 0 & 0 \end{bmatrix}
$$

satisfy the assumption (2.2).

By solving the LMI (3.23) with the help of the MATLAB toolbox, a type of feasible solution is attained as follows:

$$
\lambda_1 = 0.1295, \quad \lambda_2 = 0.1295, \quad \lambda_3 = 0.1130, \quad \lambda_4 = 0.0332,
$$

$$
X_1 = X_2 = \begin{bmatrix} 0.0086 & -0.0030 \\ 0.0085 & -0.0030 \\ 0.0085 & -0.0030 \end{bmatrix},
$$

which further implies the gain matrices of the state estimator (2.9)

$$
K_1 = K_2 = \begin{bmatrix} 0.1705 & -0.0521 \\ 0.3122 & -0.1189 \\ 0.2501 & -0.0883 \end{bmatrix}.
$$

For the purpose of simulation, the initial conditions of the states and the estimates are chosen as $x_i(0) = [0.1 \quad 0.1 \quad 0.1]^T$ and $\hat{x}_i(0) = [0 \quad 0 \quad 0]^T$ for $i = 1,2,3,4$. The initial values of the internal dynamic variable are taken as $\rho_0^1 = \rho_0^2 = 1$. The simulation results are shown in Figures 1–4. To be more specific, Figure 1 shows the occurrence instants of deception attacks and DoS attacks. The net nodes 1 and 2 are selected to be implement the event-triggered strategy. The release instants of DETM and SETM are described in the Figure 2 from which we note the transmission frequency of output signals is reduced dramatically. Figure 3 shows the estimation errors tend to a small domain of zero rather than converge to zero due to bounded perturbations, which indicates the dynamics of the augmented estimation error system achieve the desired EMSUB performance. Figure 4 depicts the evolution of the root mean square error of the augmented estimation error system. Table 1 presents the triggering rates of nodes 1 and 2 under different parameter selections for δ_i $(i = 1,2)$. The trigger rates are observed to show a consistent increase as the parameters δ_i $(i = 1,2)$ increase. In particular, according to (2.4), the DETM will reduce to the SETM when $\delta_i \to +\infty$. Thus, both Table 1 and Figure 2 demonstrate that the DETM can reduce the frequency of triggers more effectively compared to the SETM. The simulation result has verified the efficiency of the implemented DETM.

Table 1. Triggering frequencies with different threshold parameters.

Values of δ_i	Triggering of Node1	Triggering of Node2
$\delta_1 = \delta_2 = 12$	20%	10%
$\delta_1 = \delta_2 = 80$	30%	16.7%
$\delta_1 = \delta_2 = 280$	43.3%	23.3%
Static event-triggered case	80%	40%

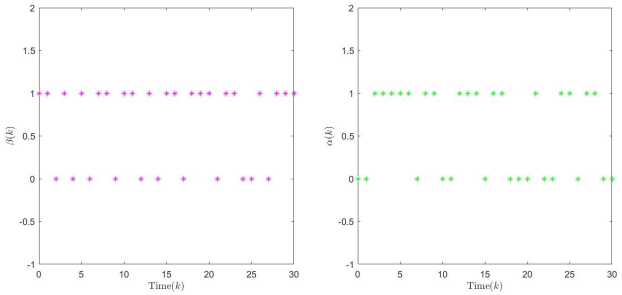

Figure 1. Occurrence of the deception attacks and DoS attacks.

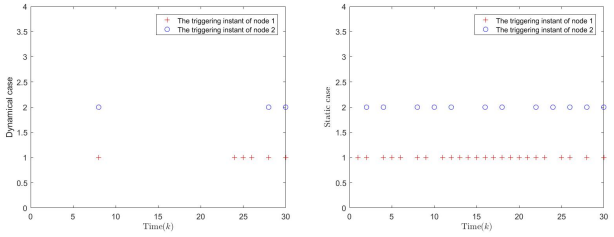

Figure 2. Dynamic and static triggering instants for nodes $i = 1,\ 2$.

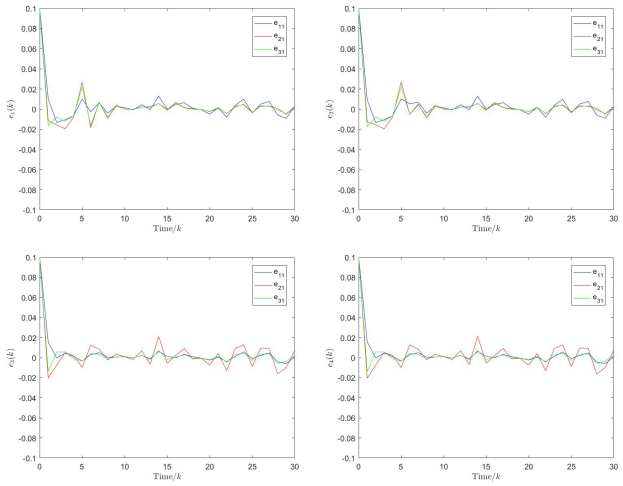

Figure 3. The estimation errors of four nodes.

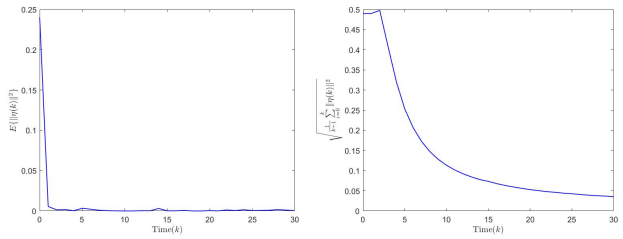

Figure 4. Square of the norm and the root mean squared error of $\eta(k)$.

5. Conclusions

In this work, we addressed the PNBSE issue for CNs subjected to hybrid cyberattacks including both DoS and deception attacks. An innovative state estimator was designed by taking use of data from selected network nodes. The DETM was applied in the data transmission process between sensors and their respective state estimators, enhancing communication resource efficiency. A comprehensive condition was established to ensure the estimation error dynamics meet the EMSUB performance. Furthermore, we derived the state estimate gain matrices by solving LMIs. The efficacy of our proposed estimation method was validated through a numerical simulation. In the future, our research will concentrate on exploring potent optimization techniques to further refine state estimation performance.

Use of Generative-AI tools declaration

The authors declare they have not used Artificial Intelligence (AI) tools in the creation of this article.

Acknowledgments

The authors would like to express their sincere thanks to the Editor and anonymous reviewers for their helpful comments and suggestions. This work was partially supported by the National Natural Science Foundation of China under Grants 62273066 and 62276034, the Natural Science Foundation of Chongqing under Grant CSTB2023NSCQ-LZX0092, and the Joint Training Base Construction Project for Graduate Students in Chongqing under Grant JDLHPYJD2021016.

Conflict of interest

All authors declare that there are no conflicts of interest in this paper.

References

1. S. H. Strogatz, Exploring complex networks, *Nature*, **410** (2001), 268–276. https://doi.org/10.1038/35065725
2. H. Dong, Z. Wang, F. E. Alsaadi, B. Ahmad, Event-triggered robust distributed state estimation for sensor networks with state-dependent noises, *Int. J. General Syst.*, **44** (2015), 254–266. https://doi.org/10.1080/03081079.2014.973726
3. H. Liu, Z. Wang, B. Shen, X. Liu, Event-triggered H_∞ state estimation for delayed stochastic memristive neural networks with missing measurements: the discrete time case, *IEEE T. Neural Netw. Learn. Syst.*, **29** (2018), 3726–3737. https://doi.org/10.1109/TNNLS.2017.2728639
4. S. V. Vasaikar, B. Jayaram, J. Gomes, B. Jayaram, Rapid computation and interpretation of Boolean attractors in biological networks, *J. Complex Netw.*, **3** (2015), 147–157. https://doi.org/10.1093/comnet/cnu011

5. R. M. D'Souza, M. Bernardo, Y. Y. Liu, Controlling complex networks with complex nodes, *Nat. Rev. Phys.*, **5** (2023), 250–262. https://doi.org/10.1038/s42254-023-00566-3

6. D. A. Burbano, G. Russo, M. Bernardo, Pinning controllability of complex network systems with noise, *IEEE T. Control Netw. Syst.*, **6** (2019), 874–883. https://doi.org/10.1109/TCNS.2018.2880300

7. I. Macaluso, C. Galiotto, N. Marchetti, L. Doyle, A complex systems science perspective on wireless networks, *J. Syst. Sci. Complex*, **29** (2016), 1034–1056. https://doi.org/10.1007/s11424-016-4122-8

8. X. Wan, Z. Wang, M. Wu, X. Liu, H_∞ state estimation for discrete-time nonlinear singularly perturbed complex networks under the round-robin protocol, *IEEE T. Neural Netw. Learn. Syst.*, **30** (2019), 415–426. https://doi.org/10.1109/TNNLS.2018.2839020

9. T. Fang, J. Sun, Further Investigate the stability of complex-valued recurrent neural networks with time-delays, *IEEE T. Neural Netw. Learn. Syst.*, **25** (2014), 1709–1713. https://doi.org/10.1109/TNNLS.2013.2294638

10. X. Yang, J. Lam, D. W. C. Ho, Z. Feng, Fixed-time synchronization of complex networks with impulsive effects via nonchattering control, *IEEE T. Automat Control*, **62** (2017), 5511–5521. https://doi.org/10.1109/TAC.2017.2691303

11. H. Rao, L. Zhao, Y. Xu, Z. Huang, R. Lu, Quasisynchronization for neural networks with partial constrained state information via intermittent control approach, *IEEE T. Cybernetics*, **52** (2022), 8827–8837. https://doi.org/10.1109/TCYB.2021.3049638

12. Y. Chen, Z. Wang, B. Shen, H. Dong, Exponential synchronization for delayed dynamical networks via intermittent control: dealing with actuator saturations, *IEEE T. Neural Netw. Learn. Syst.*, **30** (2019), 1000–1012. https://doi.org/10.1109/TNNLS.2018.2854841

13. Y. Wang, H. Liu, H. Tan, An overview of filtering for sampled-data systems under communication constraints, *Int. J. Netw. Dyn. Intell.*, **2** (2023), 100011. https://doi.org/10.53941/ijndi.2023.100011

14. Y. A. Wang, B. Shen, L. Zou, Q. L. Han, A survey on recent advances in distributed filtering over sensor networks subject to communication constraints, *Int. J. Netw. Dyn. Intell.*, **2** (2023), 100007. https://doi.org/10.53941/ijndi0201007

15. H. Peng, B. Zeng, L. Yang, Y. Xu, R. Lu, Distributed extended state estimation for complex networks with nonlinear uncertainty, *IEEE T. Neural Netw. Learn. Syst.*, **34** (2023), 5952–5960. https://doi.org/10.1109/TNNLS.2021.3131661

16. M. Zhang, X. Yang, Q. Qi, J. H. Park, State estimation of switched time-delay complex networks with strict decreasing LKF, *IEEE T. Neural Netw. Learn. Syst.*, **35** (2024), 10451–10460. https://doi.org/10.1109/TNNLS.2023.3241955

17. F. Yang, Q. L. Han, Y. Liu, Distributed H_∞ state estimation over a filtering network with time-varying and switching topology and partial information exchange, *IEEE T. Cybernetics*, **49** (2019), 870–882. https://doi.org/10.1109/TCYB.2017.2789212

18. X. Wan, Z. Wang, Q. L. Han, M. Wu, A recursive approach to quantized H_∞ state estimation for genetic regulatory networks under stochastic communication protocols, *IEEE T. Neural Netw. Learn. Syst.*, **30** (2019), 2840–2852. https://doi.org/10.1109/TNNLS.2018.2885723

19. J. Hu, Z. Wang, S. Liu, H. Gao, A variance-constrained approach to recursive state estimation for time-varying complex networks with missing measurements, *Automatica*, **64** (2016), 155–162. https://doi.org/10.1016/j.automatica.2015.11.008

20. Y. Liu, Z. Wang, Y. Yuan, F. E. Alsaadi, Partial-nodes-based state estimation for complex networks with unbounded distributed delays, *IEEE T. Neural Netw. Learn. Syst.*, **29** (2018), 3906–3912. https://doi.org/10.1109/TNNLS.2017.2740400

21. N. Hou, Z. Wang, D. W. C. Ho, H. Dong, Robust partial-nodes-based state estimation for complex networks under deception attacks, *IEEE T. Cybernetics*, **50** (2020), 2793–2802. https://doi.org/10.1109/TCYB.2019.2918760

22. J. Y. Li, Z. Wang, R. Lu, Y. Xu, Partial-nodes-based state estimation for complex networks with constrained bit rate, *IEEE T. Netw. Sci. Eng.*, **8** (2021), 1887–1899. https://doi.org/10.1109/TNSE.2021.3076113

23. N. Hou, J. Li, H. Liu, Y. Ge, H. Dong, Finite-horizon resilient state estimation for complex networks with integral measurements from partial nodes, *Sci. China Inf. Sci.*, **65** (2022), 132205. https://doi.org/10.1007/s11432-020-3243-7

24. M. Lin, Q. Shen, C. Liu, H. Peng, Y. Xu, Partial-node-based resilient set-membership filtering for output-coupled complex networks with event-triggered mechanisms, *Int. J. Robust Nonlinear Control*, **34** (2024), 5555–5569. https://doi.org/10.1002/rnc.7268

25. L. Zou, Z. Wang, J. Hu, H. Dong, Partial-node-based state estimation for delayed complex networks under intermittent measurement outliers: a multiple-order-holder approach, *IEEE T. Neural Netw. Learn. Syst.*, **34** (2023), 7181–7195. https://doi.org/10.1109/TNNLS.2021.3138979

26. N. Hou, H. Dong, W. Zhang, Y. Liu, F. E. Alsaadi, Event-triggered state estimation for time-delayed complex networks with gain variations based on partial nodes, *Int. J. General Syst.*, **47** (2018), 477–490. https://doi.org/10.1080/03081079.2018.1462352

27. Y. Deng, Z. Meng, H. Lu, Adaptive event-triggered state estimation for complex networks with nonlinearities against hybrid attacks, *AIMS Math.*, **7** (2022), 2858–2877. https://doi.org/10.3934/math.2022158

28. J. Chen, D. Yue, C. Dou, S. Weng, X. Xie, Y. Li, Static and dynamic event-triggered mechanisms for distributed secondary control of inverters in low-voltage islanded microgrids, *IEEE T. Cybernetics*, **52** (2022), 6925–6938. https://doi.org/10.1109/TCYB.2020.3034727

29. M. Shen, S. Yan, G. Zhang, A new approach to event-triggered static output feedback control of networked control systems, *ISA Trans.*, **65** (2016), 468–474. https://doi.org/10.1016/j.isatra.2016.08.014

30. J. Sun, B. Shen, Y. Liu, F. E. Alsaadi, Dynamic event-triggered state estimation for time-delayed spatial-temporal networks under encoding-decoding scheme, *Neurocomputing*, **500** (2022), 868–876. https://doi.org/10.1016/j.neucom.2022.05.062

31. F. Han, Z. Wang, H. Dong, F. E. Alsaadi, K. H. Alharbi, A local approach to distributed H_∞-consensus state estimation over sensor networks under hybrid attacks: dynamic event-triggered scheme, *IEEE T. Signal Inf. Process. Netw.*, **8** (2022), 556–570. https://doi.org/10.1109/TSIPN.2022.3182273

32. Y. Niu, L. Sheng, M. Gao, D. Zhou, Dynamic event-triggered state estimation for continuous-time polynomial nonlinear systems with external disturbances, *IEEE T. Ind. Inform.*, **17** (2021), 3962–3970. https://doi.org/10.1109/TII.2020.3015004

33. Q. Li, Z. Wang, J. Hu, W. Sheng, Simultaneous state and unknown input estimation for complex networks with redundant channels under dynamic event-triggered mechanisms, *IEEE T. Neural Netw. Learn. Syst.*, **33** (2022), 5441–5451. https://doi.org/10.1109/TNNLS.2021.3070797

34. Z. Han, S. Zhang, Z. Jin, Y. Hu, Secure state estimation for event-triggered cyber-physical systems against deception attacks, *J. Franklin Inst.*, **359** (2022), 11155–11185. https://doi.org/10.1016/j.jfranklin.2022.10.049

35. H. Sang, J. Zhao, Input-output finite-time estimation for complex networks with switching topology under dynamic event-triggered transmission, *IEEE T. Syst. Man Cybern.: Syst.*, **51** (2021), 6513–6522. https://doi.org/10.1109/TSMC.2019.2963411

36. J. Cheng, L. Liang, J. H. Park, H. Yan, K. Li, A dynamic event-triggered approach to state estimation for switched memristive neural networks with nonhomogeneous sojourn probabilities, *IEEE T. Circuits Syst. I*, **68** (2021), 4924–4934. https://doi.org/10.1109/TCSI.2021.3117694

37. S. Fan, H. Yan, X. Zhan, G. Zhou, K. Shi, Distributed set-membership estimation for state-saturated systems with mixed time-delays via a dynamic event-triggered scheme, *J. Franklin Inst.*, **358** (2021), 10079–10094. https://doi.org/10.1016/j.jfranklin.2021.08.035

38. Y. Liu, Z. Wang, Y. Yuan, W. Liu, Event-triggered partial-nodes-based state estimation for delayed complex networks with bounded distributed delays, *IEEE T. Syst. Man Cybern.: Syst.*, **49** (2019), 1088–1098. https://doi.org/10.1109/TSMC.2017.2720121

39. N. Lin, D. Chen, J. Hu, C. Jia, Partial-nodes-based state estimation for stochastic coupled complex networks with random sensor delay: an event-triggered communication method, *Circuits Syst. Signal Process.*, **41** (2022), 5461–5491. https://doi.org/10.1007/s00034-022-02059-7

40. H. Tao, H. Tan, Q. Chen, H. Liu, J. Hu, H_∞ state estimation for memristive neural networks with randomly occurring DoS attacks, *Syst. Sci. Control Eng.*, **10** (2022), 154–165. https://doi.org/10.1080/21642583.2022.2048322

41. Y. Sun, X. Tian, G. Wei, Finite-time distributed resilient state estimation subject to hybrid cyber-attacks: a new dynamic event-triggered case, *Int. J. Syst. Sci.*, **53** (2022), 2832–2844. https://doi.org/10.1080/00207721.2022.2083256

42. G. Bao, L. Ma, X. Yi, Recent advances on cooperative control of heterogeneous multi-agent systems subject to constraints: a survey, *Syst. Sci. Control Eng.*, **10** (2022), 539–551. https://doi.org/10.1080/21642583.2022.2074169

43. X. Meng, Y. Chen, L. Ma, H. Liu, Protocol-based variance-constrained distributed secure filtering with measurement censoring, *Int. J. Syst. Sci.*, **53** (2022), 3322–3338. https://doi.org/10.1080/00207721.2022.2080297

44. B. Shen, Z. Wang, D. Wang, Q. Li, State-saturated recursive filter design for stochastic time-varying nonlinear complex networks under deception attacks, *IEEE T. Neural Netw. Learn. Syst.*, **31** (2020), 3788–3800. https://doi.org/10.1109/TNNLS.2019.2946290

45. C. D. Persis, P. Tesi, Input-to-state stabilizing control under denial-of-service, *IEEE T. Automatic Control,* **60** (2015), 2930–2944. https://doi.org/10.1109/TAC.2015.2416924

46. L. Liu, L. Ma, J. Zhang, Y. Bo, Sliding mode control for nonlinear Markovian jump systems with denial-of-service attacks, *IEEE/CAA J. Automatica Sin.*, **7** (2020), 1638–1648. https://doi.org/10.1109/JAS.2019.1911531

47. M. Zhu, S. Martínez, On the performance analysis of resilient networked control systems under replay attacks, *IEEE T. Automatic Control*, **59** (2014), 804–808. https://doi.org/10.1109/TAC.2013.2279896

48. J. Liu, Y. Gu, L. Zha, Y. Liu, J. Cao, Event-triggered H_∞ load frequency control for multiarea power systems under hybrid cyber attacks, *IEEE T. Syst. Man Cybern.: Syst.*, **49** (2019), 1665–1678. https://doi.org/10.1109/TSMC.2019.2895060

49. J. Liu, M. Yang, E. Tian, J. Cao, S. Fei, Event-based security control for state-dependent uncertain systems under hybrid-attacks and its application to electronic circuits, *IEEE T. Circuits Syst. I: Reg. Papers*, **66** (2019), 4817–4828. https://doi.org/10.1109/TCSI.2019.2930572

50. Y. Chen, X. Meng, Z. Wang, H. Dong, Event-triggered recursive state estimation for stochastic complex dynamical networks under hybrid attacks, *IEEE T. Neural Netw. Learn. Syst.*, **34** (2023), 1465–1477. https://doi.org/10.1109/TNNLS.2021.3105409

51. Y. Deng, Z. Mo, H. Lu, Robust H_∞ state estimation for a class of complex networks with dynamic event-triggered scheme against hybrid attacks, *Chinese Phys. B*, **31** (2022), 269–277. https://doi.org/10.1088/1674-1056/ac0ee9

52. Y. Qu, K. Pang, State estimation for a class of artificial neural networks subject to mixed attacks: a set-membership method, *Neurocomputing*, **411** (2020), 239–246. https://doi.org/10.1016/j.neucom.2020.06.020

AIMS Press